SLAC-PUB-2010
September 1977

RELATIVISTIC INTERACTIONS BETWEEN NUCLEI, COHERENCE EFFECTS AND NONSCALING*

R. Blankenbecler and I. A. Schmidt
Stanford Linear Accelerator Center
Stanford University, Stanford, California 94305

At this moment, the most successful set of models for describing the scattering of hadrons are the relativistic hard-collision models,[1] based on a form of the impulse approximation. In this picture the colliding hadrons emit virtual subsystems, which are in the end the ones responsible for the scattering process to occur. The main theoretical points at issue are what are the dominant subsystems (quarks, gluons, hadrons, . . .) and how do they interact and scatter. There is one type of reaction in which all of the above facets are known and which should allow one to test the application and interpretation of the hard scattering formalism. These semi-gedanken experiments (they can actually be carried out!) involve relativistic interactions between nuclei, or in other words, heavy-ion reactions at high energies.[2]

In the original parton model, a hadron was considered to be a collection of elementary (pointlike) constituents called partons. This idea was based on the analogue situation in which a nucleus is composed of nucleons. We want to apply this model to the nuclear case, where it had its origins in the first place. The important point is that we can incorporate in a natural way the key elements of special relativity and nonconservation of number of particles. In addition, there is a lot known about the nuclear wave function and this can be incorporated in the treatment.

We expect this generalization to work, because in the nuclear case the characteristics of the constituents (nucleons) are well known. Thus it must work with sufficiently complicated and general wavefunctions and interactions. Our purpose is to see if a reasonably simple description of these processes can be given.

---

*Work supported by the Energy Research and Development Administration.

(Invited talk presented at the VIII International Symposium on Multiparticle Dynamics, Kaysersberg, France, June 12-17, 1977.)

One important restriction that we face is that our model must have a correct nonrelativistic limit. It must join in this limit with the usual nuclear physics description based on Schrödinger wavefunctions and interactions. This connection will provide us with useful information on the parameters of our relativistic model. It is important to stress the fact that the model contains the usual nonrelativistic results, provided appropriate wavefunctions with correct limits are incorporated. However, since we will concentrate for the most part on the kinematic regime that explores the short distance behavior of the nuclear wavefunction, we will obtain new information that is not accessible from the nonrelativistic description.

On the other hand, we can also learn how to put into the model the detailed information known about the nonrelativistic limit. These techniques may prove useful in the hadron-parton context. We will also be able to check the general features of the hard scattering model, especially the effects of coherence, and the consistency of our interpretation of the functions that enter the model. However, since the model is based on the impulse approximation, in which the effects of rescattering and shadowing are neglected, our analysis should be most applicable to light nuclei. This also means that we will not try to explain the anomalous dependence on nucleon number observed in large transverse events,[3] which is presumably connected to these effects.

One of the important lessons that we will be able to learn from the analysis of nuclear scattering is that there are terms which dominate in certain regions of phase space that correspond to the scattering of coherent subsystems emitted by the nucleus (deuterons, α-particles, etc.). It is interesting to note that in the CIM model for the scattering of hadrons,[4] this same coherence idea[5] appears, and it is quite successful in interpreting the experimental data, especially at high transverse momentum, or near the edge of phase space. We shall also apply these coherence ideas to explain (or at least to fit) the nonscaling behavior of the proton and neutron structure functions later in this talk.

Our discussion will be based in the diagram shown in Fig. 1, which represents the inclusive process $A+B \rightarrow C+X$. Here the interaction takes place through the emission of virtual subsystems (a and b), which are the ones that scatter in an internal basic process $a+b \rightarrow C+X$, where C is the detected particle. M_0 is the amplitude for this basic interaction, and the amplitudes for the emission of the a and b subsystems will be contained in distribution functions $G(x,\vec{k}_T)$, to be defined shortly. As was mentioned in the introduction, a and b may be (off-shell) nucleons or composite states that are virtually present in the nucleus, such as deuterons, alpha particles, etc... The internal amplitude M_0 will be taken from experiment, where it is given only on-shell, and extrapolated as indicated below.

The inclusive cross section is clearly of the form

$$E_C \frac{d\sigma}{d^3C} = R_C = \sum_{a,b} \int dx\, d^2k_T\, dy\, d^2\ell_T\, G_{a/A}(x,\vec{k}_T)\, G_{b/B}(y,\vec{\ell}_T)$$

$$r(s\ \ ,s,x,y) \left[E_C \frac{d\sigma}{d^3C} (a+b \rightarrow C+d;s',t',u') \right] \tag{1}$$

where

$$r = \frac{\lambda(s',k^2,\ell^2)}{xy\,\lambda(s,A^2,B^2)}$$

and where the x and y integrals run only from zero to one. The variables s', t', u' are those that describe the internal basic process and defined in terms of a, b, and C. The G functions will be defined below. The ratio r of the λ factors is the ratio of the corresponding phase space factors in the cross sections, and λ is the usual quadratic form. One finds that throughout the range of variables we are interested in, $r \approx 1$.

The interpretation of the various factors in Eq. (1) is clear. The factor $G_{a/A}(x,\vec{k}_T)$ is the probability of finding a constituent of type a in nucleus A with fractional "momentum" x and transverse momenta $\vec{k}_T$. A similar interpretation holds for $G_{b/B}$. The basic cross section factor that actually produces the detected particle C also has a clear probabilistic meaning. We have neglected final state decay to C for simplicity.

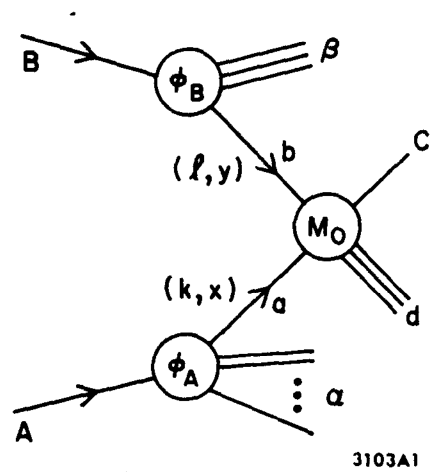

Fig. 1. The basic hard scattering model diagram with the notation used in the text.

The probability functions are defined as (see Ref. 4 for details)

$$G_{a/A}(x,\vec{k}_T) = \frac{1}{2(2\pi)^3}\frac{x}{(1-x)}\,|\psi(x,\vec{k}_T)|^2$$

where ψ is the bound state Bethe-Salpeter wavefunction with one leg (α) on-shell.

<u>Warning</u>: The validity of the hard scattering expansion requires that the sum over a and b in the above formula be incoherent. This places restrictions on the probability functions and the intermediate states included in the sum. These are ignored by many authors, so one should be wary. It is especially easy to make a mistake in this regard when photons are treated since gauge invariance forces coherence requirements that must not be ignored (but quite often are).

One can also derive an equation for the electromagnetic form factor of the state A in terms of ψ and the result is[4]

$$F_A\left(q_T^2\right) = \sum_a F_a(q^2)\int \frac{dx\,d^2k_T}{2(2\pi)^3}\frac{x}{(1-x)}\,\psi^*(x,\vec{k}_T)\;\psi\!\left(x,\vec{k}_T-(1-x)\vec{q}_T\right)$$

where the integral multiplying F_a is the body form factor of the nucleus.

We will see in our analysis that the distribution functions are explicitly measured in the experiments we are considering. For this reason it is important to have a reasonably good prediction or description of their properties. We will analyze these functions in detail, trying to get information about them from limiting cases, like the nonrelativistic and the short distance behaviors.

We will demand that when the energies and momenta are small, our description joins smoothly onto the familiar nonrelativistic treatments. In particular, the G function must be closely related in this limit with the square of the nonrelativistic wavefunction. This requirement will allow us to achieve a clearer understanding of these functions and their expected behavior, and also to explore the way masses should enter into our formalism.

First we want to see the meaning of the x-variable in a nonrelativistic limit. For momenta small with respect to the masses, and in the rest frame of the nucleus, we expect that x is directly related to the longitudinal momentum, measuring deviations with respect to a central value. In other words, each nucleon carries the same fraction of the total momentum of the nucleus. A very reasonable result in the weak binding limit.

Remember also that G is the probability of finding a constituent of A with longitudinal momentum x and transverse momentum $\vec{k}_T$. This means that G must have a maximum at $x \simeq \frac{a}{A}$, the average nucleon longitudinal momentum, and at $\vec{k}_T = 0$. Consider the definition of G, and using the Bethe-Salpeter equation we see that

$$G \sim \frac{\phi^2 x(1-x)}{\left[k_T^2 + M^2(x)\right]^2} \quad ,$$

where we have defined ϕ as the vertex function and

$$M^2(x) \equiv (1-x)(a^2-k^2) - k_T^2 = (1-x)a^2 + x\alpha^2 - x(1-x)A^2 \quad .$$

This form implies that G has a maximum at $\vec{k}_T = 0$ and at $x=x_0$, where $M^2(x)$ is a minimum. We find

$$x_0 = \frac{A^2 + a^2 - \alpha^2}{2A^2} \cong \frac{a}{A} \quad ,$$

and as expected, the constituents prefer to share the momentum according to their mass.

In the limit of small momenta one then finds with $x = (a+kz)/A$, that G becomes

$$G \equiv |\psi_{NR}(\vec{k})|^2 \sim \frac{\phi_{NR}^2(\vec{k})}{[a\epsilon + \vec{k}^2]^2} \quad ,$$

where

$$\phi_{NR}^2 \sim x_0(1-x_0)\phi^2 \quad .$$

In order to have a better understanding of the function ϕ_{NR}, consider the Schrödinger equation in momentum space

$$\psi_{NR}(\vec{k}) = (a\epsilon+\vec{k}^2)^{-1}\int d^3p\, V(\vec{k}-\vec{p})\,\psi_{NR}(\vec{p}) \equiv (a\epsilon+\vec{k}^2)^{-1}\,\phi_{NR}(\vec{k}) \quad ,$$

so that the vertex function expresses more or less directly the behavior of the potential V. The falloff of ϕ is related to the softness (or hardness) of the potential. As a simple example consider a general Hulthen model of the nuclear wavefunction:

$$\psi_{NR} = (a\epsilon+\vec{k}^2)^{-1}\left(a\epsilon_1+\vec{k}^2\right)^{\frac{1-g}{2}} \quad ,$$

where for the familiar Hulthen deuteron case, one usually chooses g=3, $\epsilon_1 \sim 36\epsilon$. The second factor is then much flatter in $\vec{k}^2$ than the first.

A relativistic version of this wavefunction can be achieved by writing

$$\psi = N(x)\,(k^2-a^2)^{-1}\left(k_1^2-a_1^2\right)^{-(g-1)/2} \quad ,$$

where N(x) is slowly varying for x near 1, and by choosing

$$(1-x)\left(a_1^2-k_1^2\right) = M^2(x) + \delta^2 + k_T^2 \equiv M_1^2(x) + k_T^2 \quad ,$$

since $M_1^2(x)$ must have a minimum in the same place as $M^2(x)$ (namely at $x=x_0$).

The form factor for this type of wavefunction is easily seen to fall as

$$F^2\left(q_T^2\right) \sim \left(q_T^2\right)^{-g-1}$$

for large q_T^2. Thus the falloff of the form factor and the behavior of G for large k_T^2 are closely related and also we see that the behavior of G for $x \sim 1$ is closely related to the form factor falloff. This latter relation is the Drell-Yan-West relation.[6]

For general x, the relativistic G function can then be written as[7]

$$G(x,\vec{k}_T) = \frac{N^2(x)\;x(1-x)^g}{2(2\pi)^3}\left[M^2(x)+k_T^2\right]^{-2}\left[M_1^2(x)+k_T^2\right]^{1-g}$$

For $x \sim x_0$, the denominator factors are rapidly varying and as has been discussed, this reduces to a familiar nonrelativistic Hulthen form. For $x >> x_0$, the numerator factors control the behavior of G, and

$$G(x,\vec{k}_T) \sim (1-x)^g$$

while its large k_T^2 behavior is $\left(k_T^2\right)^{-g-1}$.

In our analysis, the behavior of G for $x >> x_0$ will be especially important. Note that this is new information not directly contained in the nonrelativistic wavefunction. We shall also discuss quasielastic scattering which explores the G function for $x \sim x_0$ as well. Let us now turn to a discussion of the calculation of the power g in selected theories of the nucleon-nucleon interaction.

In this paragraph, the choice of appropriate wavefunctions will be discussed. A helpful tool for expressing the predictions of specific theories is in terms of "counting rules". These allow one to characterize the asymptotic behavior of G in terms of the number of constituents and the basic interactions of the theory.

Our procedure here is to extract the leading behavior from the lowest order diagram in perturbation theory. For "soft" theories, one can show that the higher orders either are small compared to the leading term or have the same behavior. (Scalar particles are assumed here for simplicity.) I shall skip details at this point; the results are physically reasonable and are no surprise. For the general structure functions $G_{a/A}$, where the state a is a bound state of <u>a</u> nucleons, the analysis can be carried through. One finds in this case

$$g = 2T(A-a) - 1$$

where T is a parameter depending upon the theory. <u>We have assumed full breakup</u> of the nucleus after a is extracted. If this is not the case, one expects the power g to be reduced (perhaps A should be the "effective number of fragments" of the residual nucleus.

The parameter T is 1 if the basic nucleon-nucleon interaction is renormalizable[8] (i.e., vector exchange with no form factors). If the vector mesons couple to the nucleons with monopole form factors (as vector dominance theories would require), then T=3. Thus T can take on any value in the above range. Note that T=3 is the same as quark counting in a renormalizable theory.[9]

Now that it is clear that one can differentiate between theories of the nucleon force by extracting values of g from the data, let us turn to a more detailed discussion of the probability functions. The G's that will be considered here are all of the form

$$G_{a/A}(x, \vec{k}_T) = \frac{1}{2(2\pi)^3} \frac{N^2(x)\, x(1-x)^g}{\left[k_T^2+M^2(x)\right]^2 \left[k_T^2+M_1^2(x)\right]^{g-1}}$$

where N(x) is a slowly varying function of x, and

$$M^2(x) = (1-x)a^2 + x\alpha^2 - x(1-x)A^2$$

$$M_1^2(x) = M^2(x) + \delta^2 \quad .$$

This general form for G has several properties that are work noting:

- G is peaked at $k_T=0$ and the transverse momentum distribution falls more and more rapidly as A increases.
- G is peaked at $x \sim a/A$. The most likely momentum configuration is that one in which the nucleons share equally the total momentum of the nucleus.
- The power g which controls both $x \sim 1$ and large k_T is very simple to characterize in terms of the basic binding interaction and the number of constituents.
- The shape of G in the nonrelativistic limit does not restrict the behavior for $x \sim 1$ for general models (although they are strongly correlated in our simple models). A measurement of G for $x \sim 1$

is new information that is not accessible to conventional nuclear theory.

In order to get simple predictions that can easily be compared with experiment without extensive numerical calculation, we will first analyze the situation in which the energy per nucleon is large compared to the nucleon mass. The kinematics for this regime is quite simple:

$$s' = xys$$

$$t' = yt$$

$$u' = xu$$

$$d^2 = xys + yt + xu$$

and

$$C_T^2 = \frac{ut}{s} = C_T'^2$$

The condition $d^2 > 0$ restricts the range of x and y that contribute for fixed values of s, t, u.

Note that the internal reaction can be inclusive ($d^2 > 0$) or exclusive ($d^2 = 0$). This last situation is the case in quasielastic scattering, for example.

All inclusive basic processes of interest to us here will be parametrized as

$$\left[E_C \frac{d\sigma}{d^3C}\right]' = E(s')\left(1 - |x_F'|\right)^H f(k_T')$$

and exclusive processes as

$$\left[E_C \frac{d\sigma}{d^3C}\right]' = E(s')\,\delta\left[(k+\ell-C)^2 - d^2\right] f(k_T') ,$$

where $k_T' = C_T - k_T - \ell_T$ and $E(s')$ is assumed rather slowly varying. H will be assumed to be constant.

Now we will discuss the model in selected regions of phase space in which the predictions are easy to extract. First define

$$\epsilon = \frac{m^2}{s} = 1 - x_R \cong 1 - \frac{|\vec{C}_{c.m.}|}{|\vec{C}_{max}|} ,$$

where m is the full missing mass of the reaction, and

$$x_T = \frac{C_T}{C_{max}} \qquad\qquad x_R = \sqrt{x_T^2 + x_L^2}$$

$$x_L = \frac{C_L}{C_{max}} \cong \frac{t-u}{s}$$

and for the most part we will concentrate in the region where ϵ is smaller than the quasielastic peak (that is, x_R larger than the most likely value $\approx a/A$).

For an inclusive basic process, one finds in the target fragmentation region (t small, $x_F > 0$) that

$$R \sim (1-x_F)^{g_B+H+1}$$

A more accurate treatment is possible but the above will suffice for our purposes. However in the <u>target fragmentation region</u>, where us is fixed and s, t large, the result is that

$$R \sim (1+x_F)^{g_A+H+1}$$

The elastic basic process results follow by setting H=-1, but more accurately, one finds

$$R \propto G_{C/B}\left(x_F - \Delta, K^2\right)\left(\frac{d\sigma}{dt}\right)' ,$$

where Δ is a small kinematic shift that depends on the masses involved. For this case, the structure function G is directly measurable.

In general, a simple formula also holds throughout the Peyrou plot. By repeating the arguments given above with more care at general scattering angles, one finds

$$R_C = I(\epsilon)\, \epsilon^{F+1+H}\, (1-x_R z)^{-F_-}\, (1+x_R z)^{-F_+}\, J\left(C_T^2\right) ,$$

where $z = \cos\theta_{c.m.}$, $F_- = 1+g_a$, $F_+ = 1+g_b$, $F = 1+g_a+g_b$, and $I(\epsilon)$ is a slowly varying function of ϵ. This result is valid for an inclusive internal process parametrized in the form

$$R'_C \sim (1-x'_R)^H\, J\left(C'^2_T\right) \quad .$$

Although this form was derived assuming $|z|$ not near one (outside the forward and backward cones), we see that it also has the correct limit inside those regions. This expression can then be used to characterize the inclusive nuclear reaction at all angles. Furthermore, since we expect a smooth transition from the regions of validity of this form to other regions of the Peyrou plot (i.e., the central region), this equation can be used to fit the data everywhere (with effective powers).

Pion Production

As the first application of the model, we shall consider π^- production in the projectile fragmentation region for several different reactions. The small angle data in Fig. 2, taken from J. Papp et al.,[2] clearly supports the value H=3. The value of T now can be determined by looking at deuteron beam data. The fit for T=3 is compared with the data[2] in Fig. 3. Now all parameters are fixed and the prediction for alpha beams is compared with the data[2] in Fig. 4.

The proton yield in the forward and backward direction is fully determined since it depends only on T (H=-1). For these reactions the data is not as extensive in the variable x_F as in the pion data so the tests are not as severe. The reaction $d+C \rightarrow p+X$ is predicted to go as ϵ^5. The data is in reasonable agreement with this behavior but it does not fall quite this fast for the largest x_F values. The prediction for the proton yield from carbon-carbon collisions is compared with the data[2] in Fig. 5.

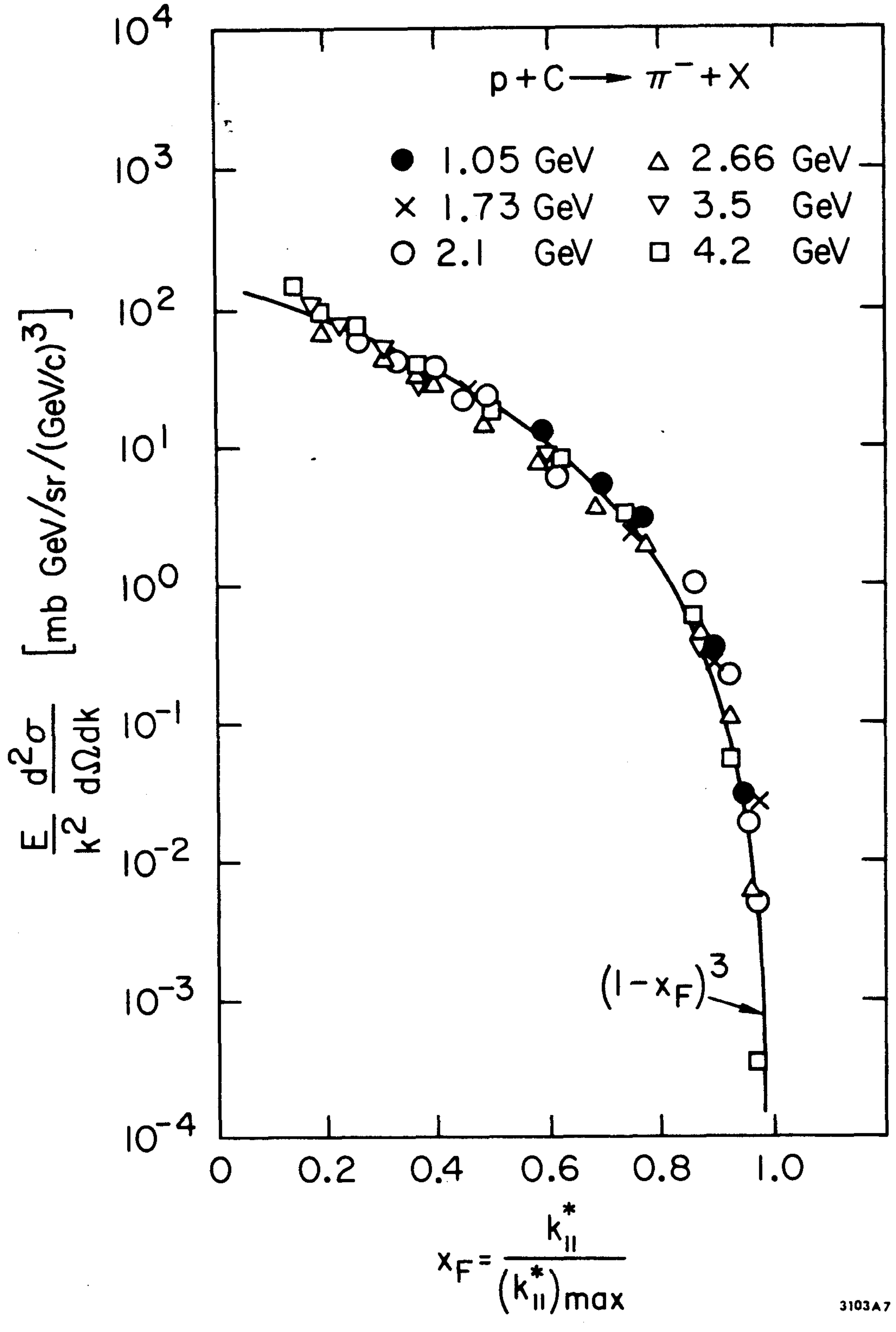

Fig. 2. The x_F spectrum compared to the carbon data illustrating scaling and the value of H.

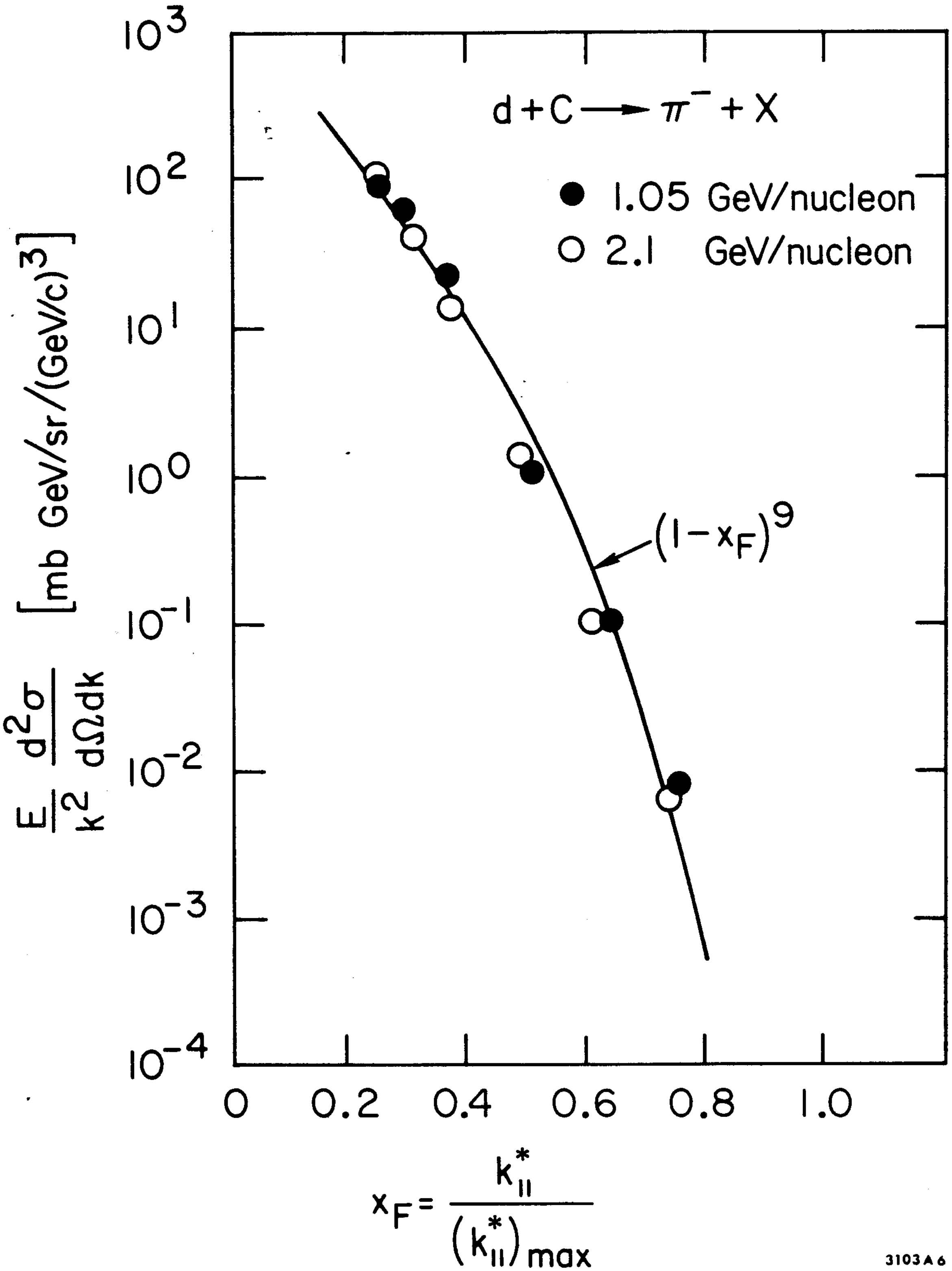

Fig. 3. The prediction for T=3 compared to the data of Ref. 2 for a deuteron beam.

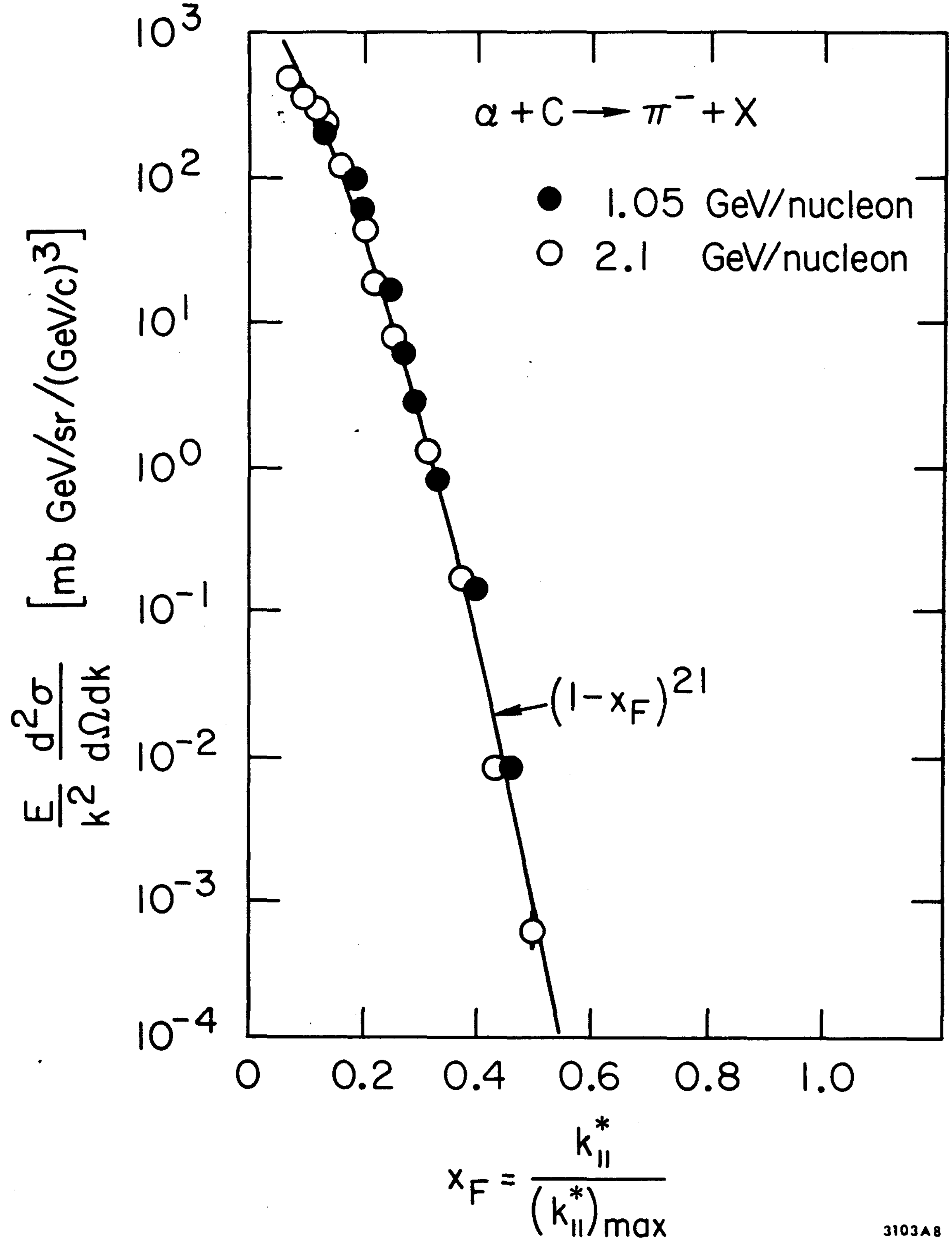

Fig. 4. The prediction for T=3 compared to the data for an alpha particle beam.

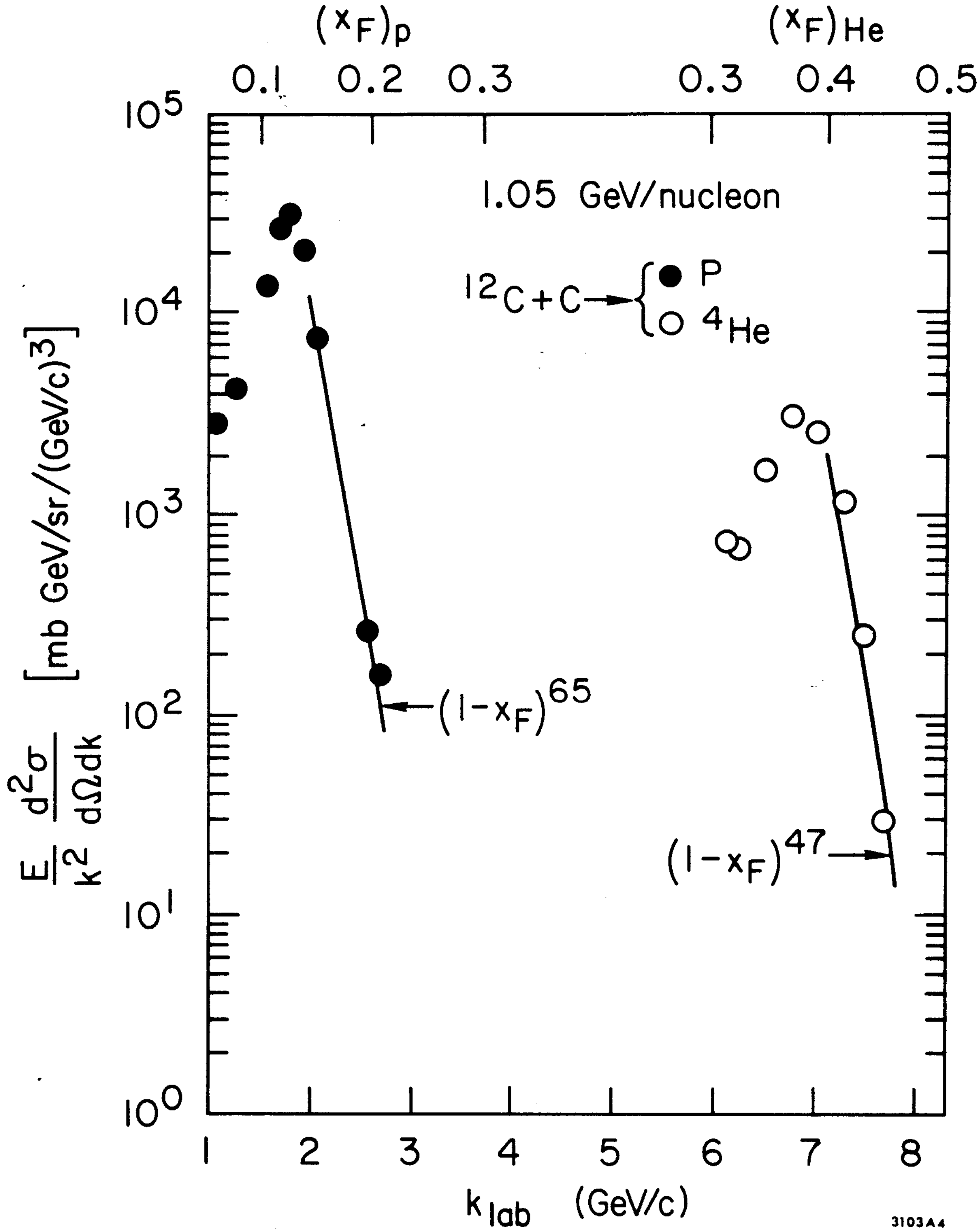

Fig. 5. Two inclusive processes for a carbon beam illustrating the counting rules and the positions of the quasielastic peaks.

Also shown is the alpha particle yield. It is clear that in this case, an important contribution is due to the incident ion splitting into α plus residue and the α scattering into the forward direction. This term yields the prediction shown in the graph. Clearly, such coherent intermediate states are important even though they are lightly bound (compared to the incident energy).

We must point out that in order to compare our simple power law predictions with experimental data, this has to be done for x_F away from quasielastic peaks (one can always use our more accurate parametrizations of G and numerically compute the yield for all x_F values), and at high energies per nucleon. This last point is worth commenting on a little more. The energy has to be high for two reasons, first so that masses can be neglected, and second so that we are sure that the nuclei in the reaction have broken apart, without leaving any nuclear bound states. A generalization that includes this last situation should not be difficult, however it will tend to reduce the predicted ϵ powers.

The effects of absorption were completely neglected in the above treatment, and this is a very important omission that must be remedied if one wishes to compute the absolute normalization of the reactions discussed here.

In conclusion, we feel that the general approach used here to describe the high energy scattering of heavy ions has many advantages over the conventional approach using Schrödinger wavefunctions and standard scattering theory but with no increase in complexity.

Let us now turn to neutrons, deuterons, and form factors. A very plausible wavefunction ψ, which we saw before gives a G function with several correct properties, is

$$\psi(x,\vec{k}_T) = \frac{N(x)(1-x)^{\frac{g+1}{2}}}{\left[k_T^2 + M^2(x)\right]\left[k_T^2 + M^2(x) + \delta^2\right]^{\frac{g-1}{2}}}$$

where for the case of the deuteron g=5 for the theory with T=3 (exchange of vector mesons with monopole form factors at each vertex). We have shown that this theory gave good results for inclusive reactions, and that this form for ψ is quite successful in reproducing quasielastic scattering data involving the deuteron. The deuteron form factor can now be computed from $\psi(x, k_T)$. A fit that can be achieved for our spinless model is given in Fig. 6 for the value $\delta^2 = 200\ M\epsilon$, where M is the nucleon mass and ϵ is the binding energy of the deuteron. Here the isoscalar form factor was taken to be equal to the proton form factor. The results are compared to selected data points[10] in Fig. 6. Now that we have some confidence in the deuteron wavefunction, it can be used to predict the deuteron structure function and used to extract the neutron structure function from the experimental data.

Our nuclear scattering analysis has shown that there are coherence effects that dominate in certain regions of phase space, and which correspond to virtual emission of nuclear bound states by the interacting nuclei. It is interesting to note that in the CIM model of hadron collisions the picture is very similar, and the interacting particles emit coherent subsystems (diquarks, mesons, baryons,...) which are the ones that give rise to the internal basic interaction. This means that there are several different terms whose relative importance will depend on the region of phase space that we are considering. In this section we will analyze deep inelastic scattering from protons and neutrons, using the same general ideas.

For deep inelastic events, that is, large energy (ν) and momentum (q^2) transfer, Bjorken predicted that the structure functions would remain finite and would depend only on a single variable $x = -q^2/2M\nu$. The approximate validity of this prediction[11] has had a considerable influence on the theory of hadrons, which most people consider today as being composite states of (almost) point-like objects, or perhaps asymptotically free objects.

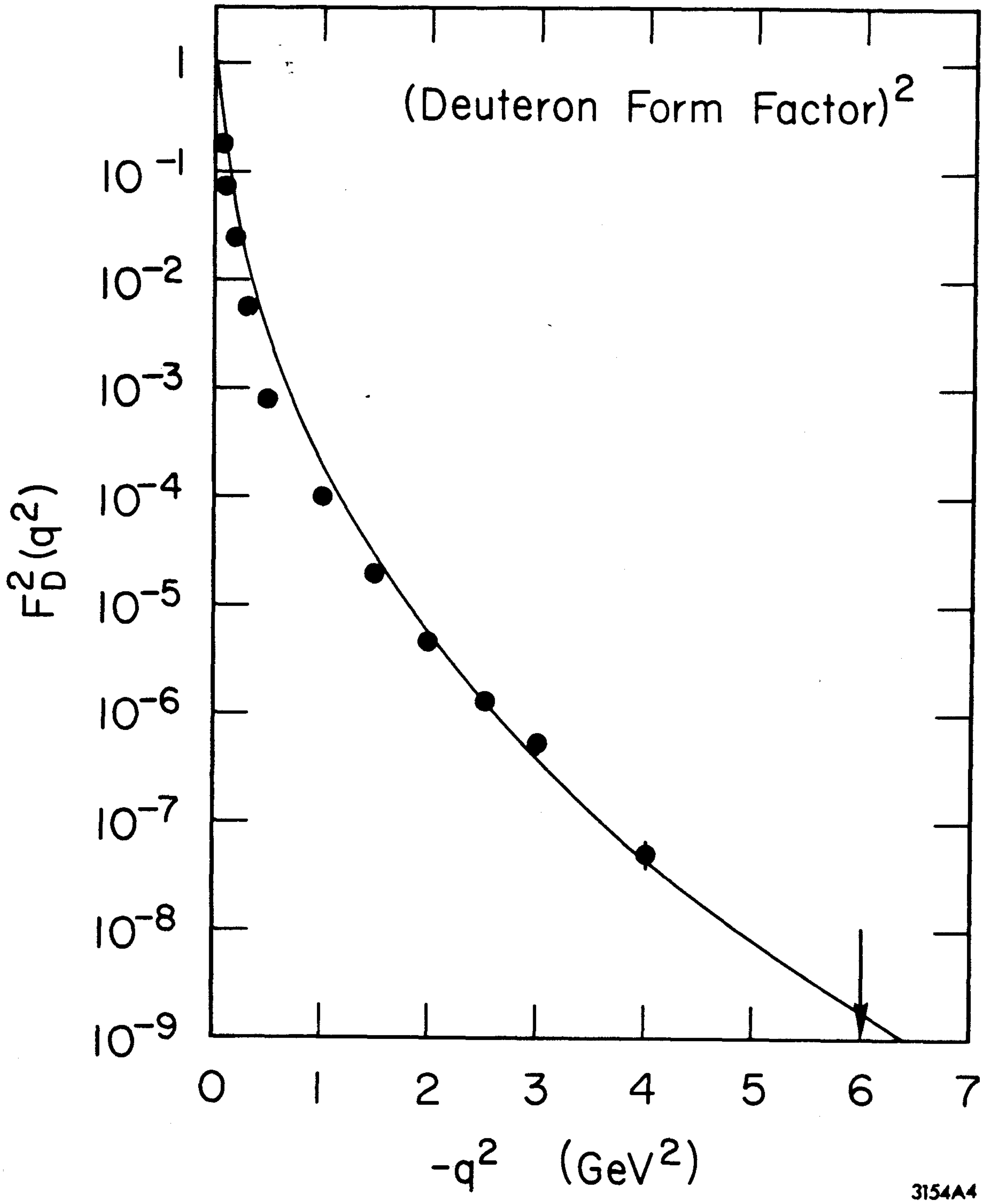

Fig. 6. Fit to the (deuteron form factor).^{2}

Let us turn first to a discussion of nonscaling terms in the parton model. Our purpose here is quite modest in comparison to the total program of the asymptotic freedom riders, for example. We only wish to point out that there are certain scale breaking effects that are very simple from a physical point of view and which would seem to be present in any theory susceptible to a parton interpretation. These terms are a priori expected to be important for large x, the Bjorken scaling variable. At small x, they do not necessarily dominate from general arguments and there are many additional effects that could become important. Indeed, the data indicates that the terms under consideration are certainly not dominant there (but simple wave-function effects may be).

These contributions show up first in the twist-6 terms in the language of the operator product expansion and would thereby be normally neglected. However they would be expected to be large from physical arguments. While they fall rapidly in q^2, their coefficient is expected to be large. They do not correspond to interference terms between various final state configurations that prefer to populate different regions of the final phase space. If such "trivial" scale breaking terms are present in the data with its necessarily finite q^2 range, it is certainly important to recognize their effect before asking more fundamental and specific questions of such data since these terms should be present in almost any theory. The inclusion of such terms in the asymptotic freedom fits should allow one to slow down the expected nonscaling (log) effects, and perhaps affect the fit to the neutrino data.

In order to separate the terms that contribute, we will follow the same classification scheme as in the deuteron case, which is based on the idea that as q^2 increases more and more substructure is revealed in the hadronic bound state. The different contributions to the structure function are most easily described in the parton-quark language. The structure functions will be written as a sum over final states in which all the quarks have low transverse momenta except for (a) one quark which recoils with momentum $\approx q$, (b) two quarks that recoil with a total of $\sim q$ but each has a finite fraction of q, (c) three quarks that recoil with a total of $\sim q$, etc. The above classification neglects the coherence between such states and should be applicable for sufficiently large q values where the final configurations become incoherent. The importance of type (b) terms, for example, will be shown to be the fact that while they fall in q^2 at fixed x, they vanish less rapidly than type (a) terms for fixed q^2 as $x \to 1$.

Using the dimensional counting rules,[8] the proton structure function is written as

$$F_{2p} = F^V_{2p}(x) + F^d_{2p}(x, q^2) + F^{sea}_{2p}(x, q^2) \quad ,$$

where the valence quark, diquark, and sea contributions are

$$F^V_{2p} = A_V(x)\ (1-x)^3$$

where $A_V(x)$ will be fit to the data, and

$$F^d_{2p}(x, q^2) = A_d F^2_d(q^2)\ x^2(1-x) \quad ,$$

where F_d is predicted to be

$$F_d(q^2) = d^2(d^2-q^2)^{-1}$$

The sea contribution is written as

$$F^{sea}_{2p}(x, q^2) = \theta(0.6 - \sqrt{x})(1-x)^7(0.6 - \sqrt{x})\left(1 - 2F^2_d(q^2)\right) \quad .$$

This latter form was fit to a calculation of the rise (as q^2 increases) found in F_2 in a detailed model of the nucleon wavefunction. These wavefunction effects are important at all x, however at large x, the diquark term dominates and leads to a net decrease with q^2. The resultant fit to proton data[12] yields the structure function[13] shown in Fig. 7.

Since the distribution function $G_{a/D}(x)$ is known with some accuracy, it will be used to extract the neutron structure function $F_{2n}(x, q^2)$ from the large q^2 deuteron

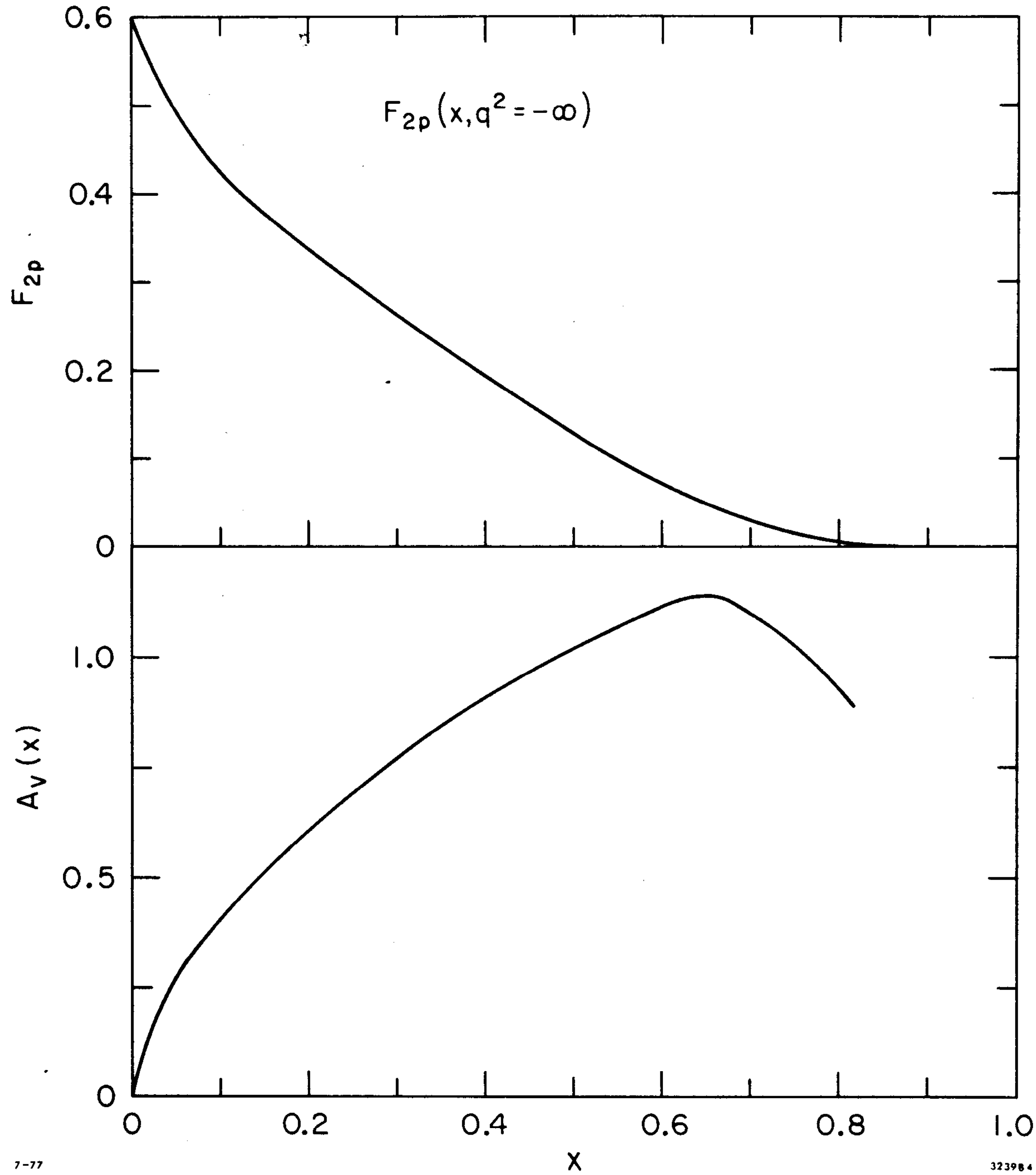

Fig. 7. Scaling part of the proton structure function ($F_{2p}(x, q^2 = -\infty)$), and coefficient $A_V(x)$ of the valence contribution.

data. In order to carry out the fit in a convenient form, we define

$$F_{2n}(x,q^2) = F_{2n}^V(x) + F_{2n}^d(x,q^2) + F_{2n}^{sea}(x,q^2) \quad ,$$

where

$$F_{2n}^V(x) = B_1(x)\, F_{2p}^V(x) \quad ,$$

$$F_{2n}^d(x,q^2) = B_2(x)\, F_{2p}^d(x,q^2) \quad ,$$

$$F_{2n}^{sea}(x,q^2) = F_{2p}^{sea}(x,q^2) \quad .$$

The resultant fit to the data is again excellent and the neutron-proton comparison is given in Fig. 8. The various contribution to the structure function are given in Fig. 9. In Fig. 10 a prediction for the changes as a function of q^2 are given. These, of course, neglect any asymptotic freedom effects. A comparison with the new muon data from FNAL will be very interesting and crucial in separating the effects due to asymptotic freedom and quark coherence.

There are several points worth mentioning. The function $B_1(x)$ is slowly varying over the range of x considered, $x > 0.1$. The average value of $B_1(x)$ around the valence peak ($x=1/3$) is roughly consistent with 2/3 which is the ratio of the sum of the squares of the valence quark charges, neutron/proton = (2/3)/1. The ratio of the asymptotic neutron to proton structure functions decreases for large x, and the extrapolation seems to give the value of $\approx 1/4$ at $x=1$, which is the lower bound that holds in the valence quark model. At $x=0$, on the other hand, this ratio goes to 1, which reflects the isoscalar character of the parton sea.

The value of 1/3 found for $B_2(x)$ is the ratio of the sum of the squares of the valence diquark charges, neutron/proton = (2/3)/3. These features of the fit are evidence of the consistency of our interpretation and fit (but certainly not its uniqueness).

To conclude, we have shown that a simple extension of the parton model, together with dimensional counting, provides a reasonable fit to the nonscaling behavior of the

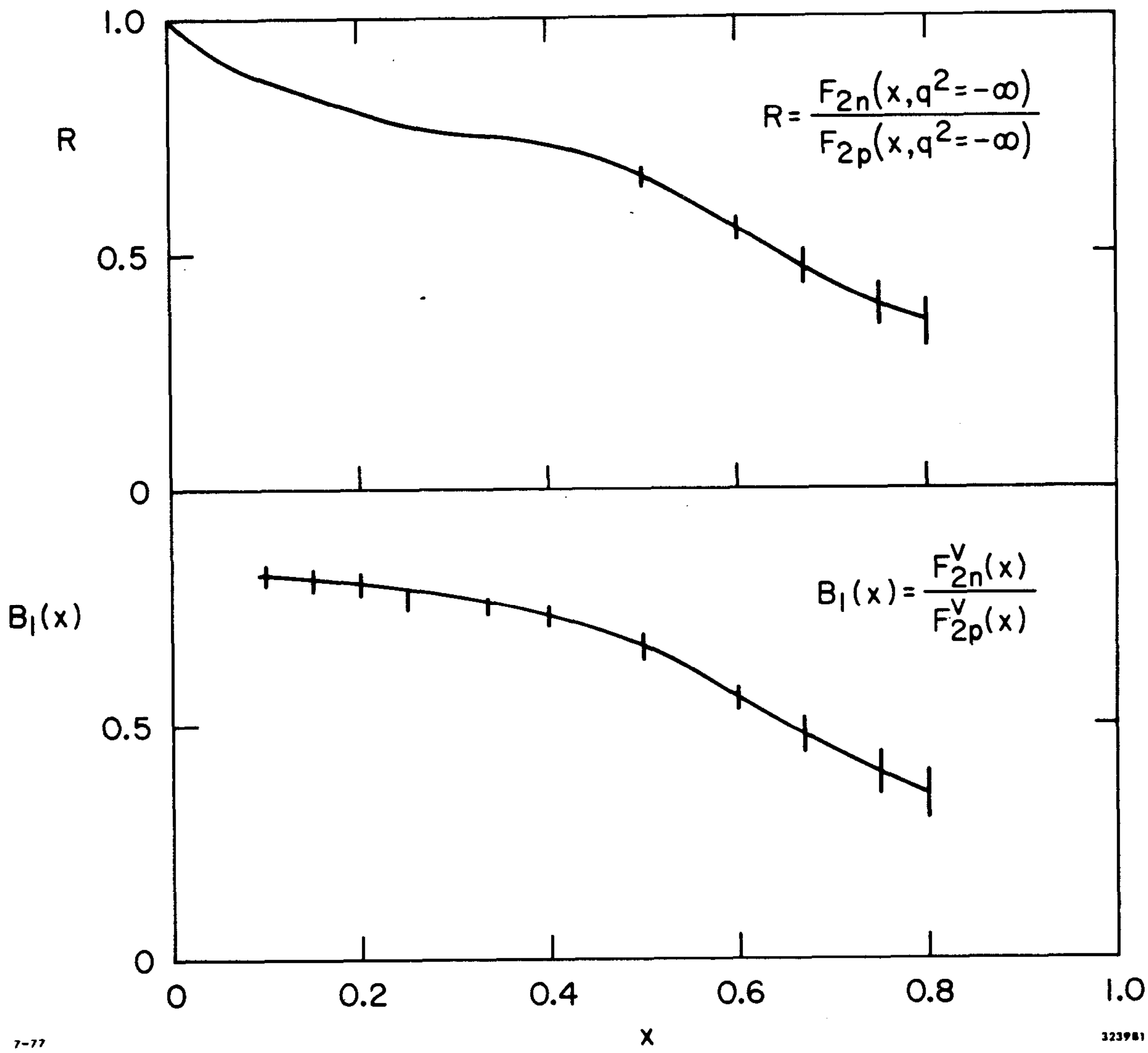

Fig. 8. Ratio of the asymptotic structure functions of proton and neutron $F_{2n}(x, q^2 = -\infty)/F_{2p}(x, q^2 = -\infty)$, and ratio of the valence parts $F_{2n}^V(x)/F_{2p}^V(x)$.

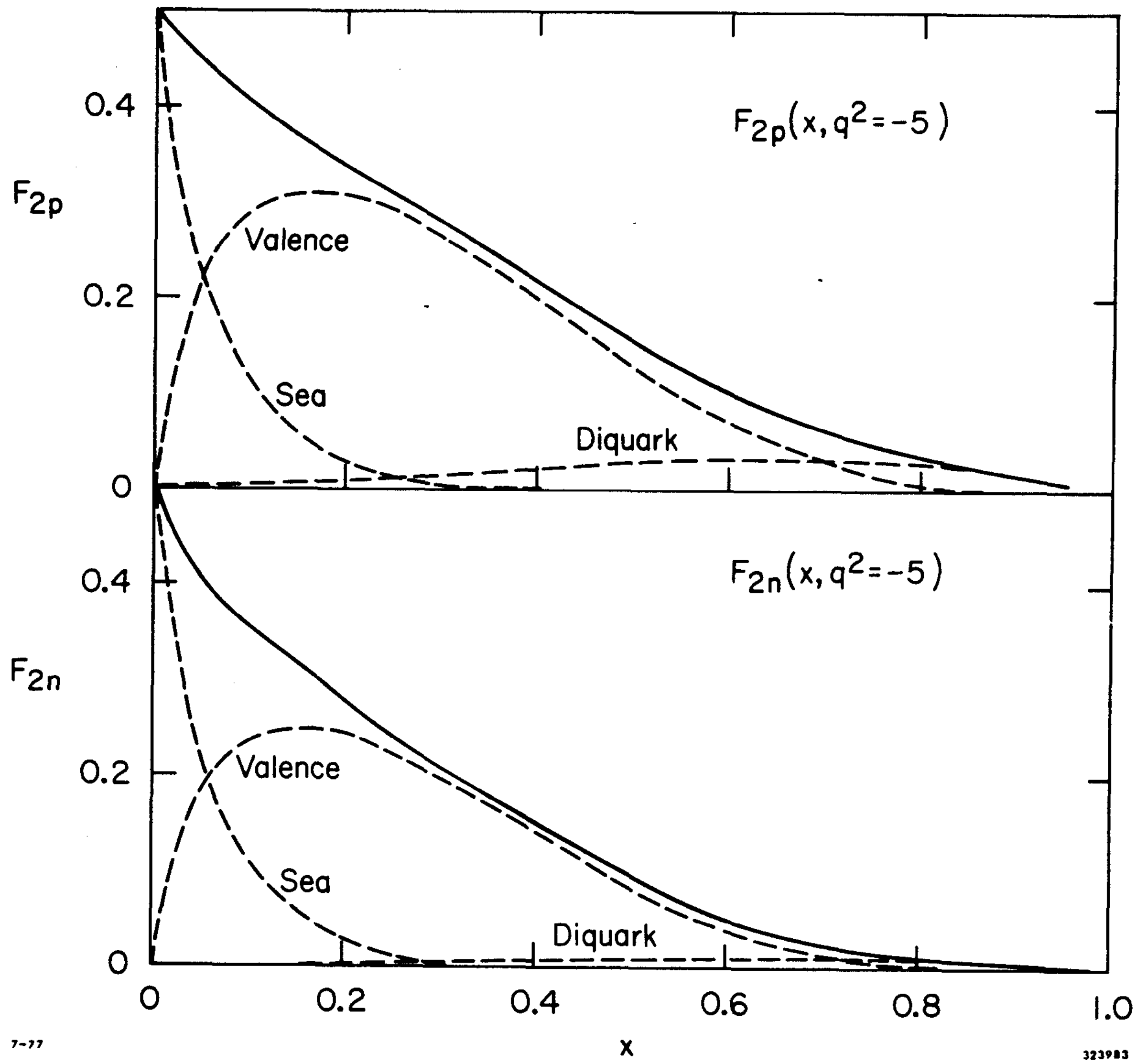

Fig. 9. The contributions (valence, diquark and sea) and the total structure functions of proton and neutron (for $q^2 = -5$ (GeV)^2).

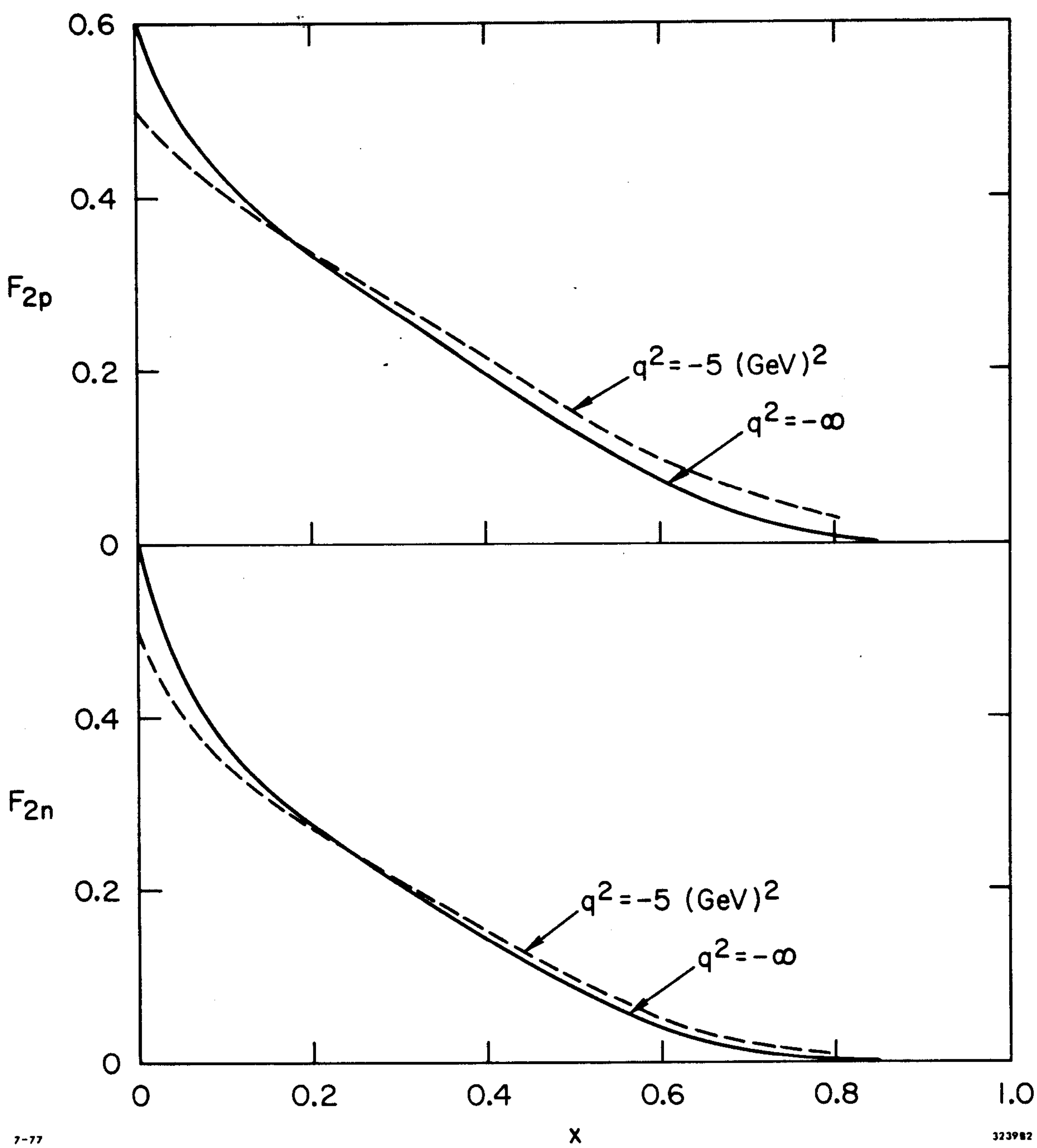

Fig. 10. The proton and neutron structure functions, for $q^2=-5$ (GeV)^2 and $q^2=-\infty$.

proton and neutron structure functions which is particularly simple for x larger than the valence quark peak at 1/3. The model can be tested by looking at the proton yield in the photon fragmentation region.[13] We therefore conclude that if one wants to differentiate between basic theories of hadrons by studying only the structure functions, it must be done at small x where the above nonscaling terms are probably unimportant. Even in this region of x, however, one is faced with the problem of demonstrating that such effects are indeed small, especially if one is making a quantitative comparison with a particular basic theory.[15]

Finally, in answer to the persistent questioning of Dave Morrison, I will show the value of $\bar{\nu}/\nu$ ratio that follows from the above model of the structure functions. The calculation by Fernandez-Pacheco, Grifols and Schmidt are given in Fig. 11 for the kinematic cuts (as we understand them) used in the HPWF data analysis.

References

1. There are too many diverse references to cite any particular group.
2. There are many references here also, but the set of experiments of most interest to us here are J. Papp et al., Phys. Rev. Letters 34, 601 (1975); J. Papp, Ph.D. Thesis, University of California, Berkeley, Report LBL-3633 (1975).
3. J. W. Cronin et al., Phys. Rev. Letters 31, 1426 (1973). J. W. Cronin et al., Phys. Rev. D 11, 3105 (1975).
4. R. Blankenbecler, S. J. Brodsky and J. F. Gunion, Phys. Rev. D 6, 2652 (1972). See also D. Sivers, S. J. Brodsky and R. Blankenbecler, Physics Reports C 23, No. 1 (1976).
5. These coherence effects are neglected in the pure parton treatment of R. D. Field and R. P. Feynman, CALT-68-565 (1977).
6. S. D. Drell and T.-M. Yan, Ann. Phys. (N.Y.) 66, 578 (1971). G. West, Phys. Rev. Lett. 24, 1206 (1970).

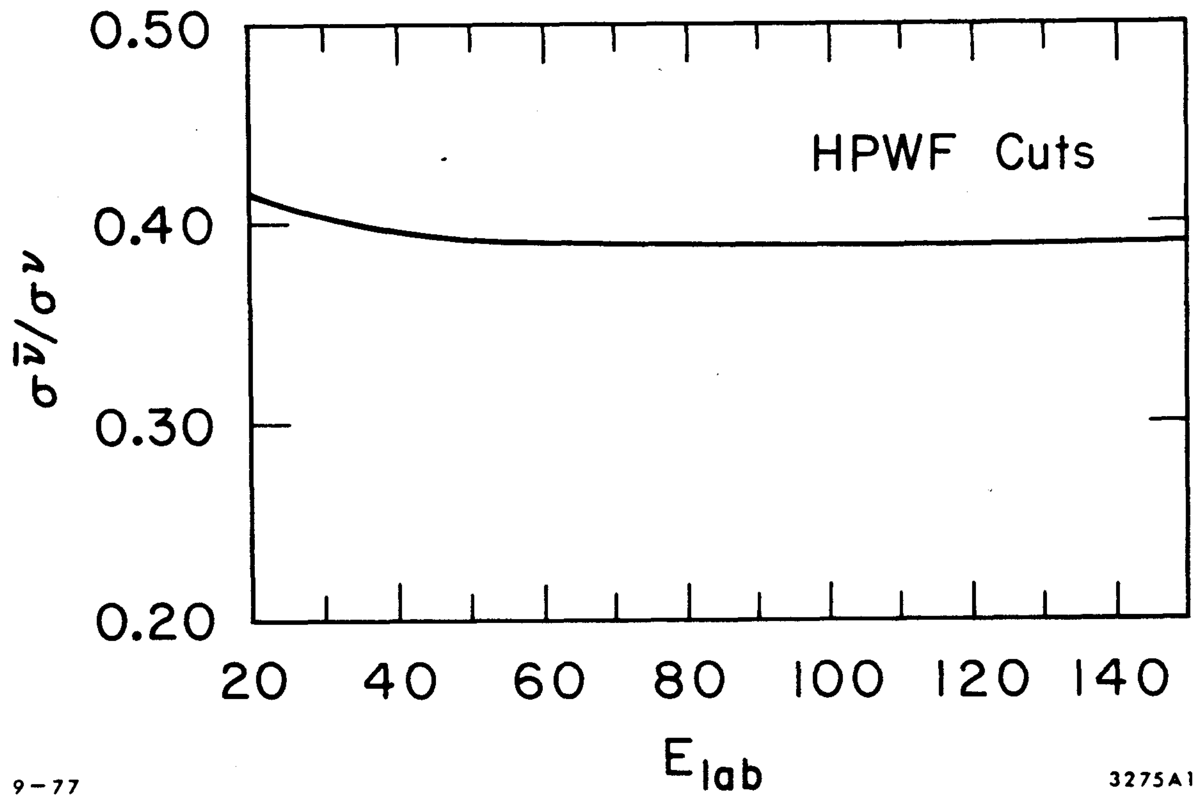

Fig. 11. The antineutrino/neutrino cross section ratio that follows from the structure functions of the text (see Ref. 14 for details). If no kinematic cuts are made, the curve drops by ≈ 0.01 only.

7. We are generalizing and improving the hadron case treatment of C. Sachrajda and R. Blankenbecler (unpublished).

8. R. Blankenbecler and S. J. Brodsky, Phys. Rev. D 10, 2973 (1974). For fixed angle counting rules see S. J. Brodsky and G. R. Farrar, Phys. Rev. Letters 31, 1153 (1973); Phys. Rev. D 11, 1309 (1975).

9. S. J. Brodsky and B. T. Chertok, Phys. Rev. D 14, 3003 (1976).

10. R. G. Arnold et al., Phys. Rev. Letters 35, 776 (1975). Lower energy data is taken from: J. Elias et al., Phys. Rev. 177, 2075 (1969); and S. Galster et al., Nucl. Phys. B32, 221 (1971).

11. R. E. Taylor, in Proceedings of the 1975 International Symposium on Lepton and Photon Interactions at High Energies, ed. by W. T. Kirk (Stanford Linear Accelerator Center, Stanford University, Stanford, California, 1975), p. 679.

12. E. M. Riordan et al., Stanford Linear Accelerator Center preprint SLAC-PUB-1634 (1975). See also J. S. Poucher et al., Phys. Rev. Letters 32, 118 (1974). Data at small x (muon scattering) is from H. L. Anderson et al., Phys. Rev. Letters 38, 1450 (1977).

13. I. A. Schmidt and R. Blankenbecler, Stanford Linear Accelerator Center preprint SLAC-PUB-1938 (1977).

14. A. Fernandez-Pacheco, J. A. Grifols and I. A. Schmidt, Stanford Linear Accelerator Center preprint SLAC-PUB-1993 (1977) (submitted to Phys. Rev. Letters).

15. See, for example, the data and asymptotic freedom fits in the following: S. J. Barish et al., ANL-HEP-PR-76-66; J. P. Berge et al., Phys. Rev. Le Letters 36, 639 (1976); H. Deden et al., Nucl. Phys. B85, 269 (1975); C. Cline, Proceedings of the Palermo Conference on High Energy Physics, 1975. A fit to some of this data has been given by V. Barger et al., Nucl. Phys. B102, 439 (1976). Further tests have been presented by R. M. Barnett and F. Martin, Stanford Linear Accelerator Center preprint SLAC-PUB-1892 (1977). A detailed fit to the new neutrino data from CERN would be very interesting.